Hot wire anemometer operating at cryogenic temperatures

B. Castaing, B. Chabaud, and B. Hébral
CNRS-CRTBT[a] BP 166, 38042 Grenoble Cédex 9, France

(Received 25 October 1991; accepted for publication 27 May 1992)

A micronic-size hot wire anemometer operating at cryogenic temperatures (4 K) has been developed; using superconducting and resistive thin films, its electrical resistance is very sensitive to the velocity of a gaseous ^{4}He subsonic jet. The fabrication procedure is described and the measured characteristics are compared with a simple thermal equilibrium model.

I. INTRODUCTION

Gaseous ^{4}He at cryogenic temperatures has already been used with some success for experiments on turbulence.[1,2] Its kinematic viscosity can be easily modulated by adjusting the pressure, going down to the lowest value of all fluids: 2×10^{-8} m^2/s, when the easily accessible critical pressure P_c (0.22 MPa) is approached. It results in two main advantages:

(1) Large values of the control parameter (Reynolds, or Rayleigh numbers for convection experiments) can be achieved with laboratory-sized, well-controlled experiments.

(2) Several decades of this control parameter can be covered in a very clean way, only by varying the pressure of the gas.

Obviously, gaseous ^{4}He experiments are not the panacea and reducing the sizes has some drawbacks. The smallest structures of the flow, which are typically 0.1–0.3 mm in size in air experiments, come down to less than 10 μ size. The typical frequencies go up from 10 kHz to 1 MHz! A good detector must then be of micronic size and have a dynamical response up to 1 MHz.

In this paper we describe the principle of such a cryogenic detector for velocity measurements, the prototype development and characterization, and its first test in a He flow.

II. THE DETECTOR PRINCIPLE

Hot wire anemometers have been used for a long time as suitable velocity detectors both in terms of size and time constant. Heated by Joule effect such a sensor is cooled by convection in the flow. Its electrical resistance, depending on the temperature, will give a measurement of the flow velocity,[3] and its low heat capacity allows a high dynamic response.

At liquid-helium temperature, the last characteristic is the easiest to fulfill as the heat capacity of every material goes to zero at low temperature. On the other hand, normal metallic wires present a temperature-independent characteristic and are no more useful detectors. We have chosen to develop a new detector type using thin films of resistive and superconducting metals deposited on a glassy micronic-size substrate. A schematic diagram of the sensor is shown in Fig. 1.

On a 5-μm-diam and 1-mm-long glass fiber, a 500-Å-thick chromium film is evaporated and covered by a 100-Å-thick noble metal (Ag or Au) layer. Another 5-μm-diam wire is then placed cross to the glass fiber in order to mask a small length during the next deposit (thickness $\sim$2500 Å) of the superconducting metal (Pb-In alloy). This uncovered section of the sensor will be the hot spot when a current is applied. Above some critical value I_l, this hot spot will warm the adjacent superconducting layer above its critical temperature T_c and the total resistance of the sensor will vary from R_0, the hot spot resistance, to R_0+R, where R is the resistance of the Pb-In alloy section in the normal state. For two different flow regimes ($v_2 > v_1$), the expected voltage current will feature as shown in Fig. 2.

We shall first discuss the static response of the wire. Its temperature profile may be determined from the local energetic equation

$$RI^2 = -K_M \frac{d^2T}{dx^2} + K_H(T-T_0). \tag{1}$$

This equation expresses the balance between the Joule heating and the cooling through the wire and the gas. T_0 is the mean temperature away from the wire. K_M is the normalized thermal conductivity along the fiber. If we neglect the thermal conductivity of the glass: $K_M = Ak_m$, where A is the cross section of the metal and k_m its thermal conductivity. The K_M values when the heat transfer along the glass fiber is taken into account are given in the discussion section. K_H is the normalized heat transfer coefficient to the gas: $K_H \sim \pi k_{\mathrm{He}}$, in the absence of flow, where k_{He} is the thermal conductivity of the gas. In the presence of flow K_H will be enhanced due to the formation of a boundary layer around the wire. In this equation K_H is thus the only velocity-dependent parameter.

Two cases have to be considered (the calculations are developed in the Appendix):

(a) $I < I_l$, no transition has occurred in the superconductor. The temperature profile in the situation of Fig. 3(a) is given by

$$T = T_1 - 2A\cosh\frac{x}{\lambda_1} \quad x < l,$$
$$T = T_0 + Be^{(l-x)/\lambda_2} \quad x \geqslant l, \tag{2}$$

[a]Associated to the University Joseph Fourier, Grenoble.

 0034-6748/92/094167-07$02.00

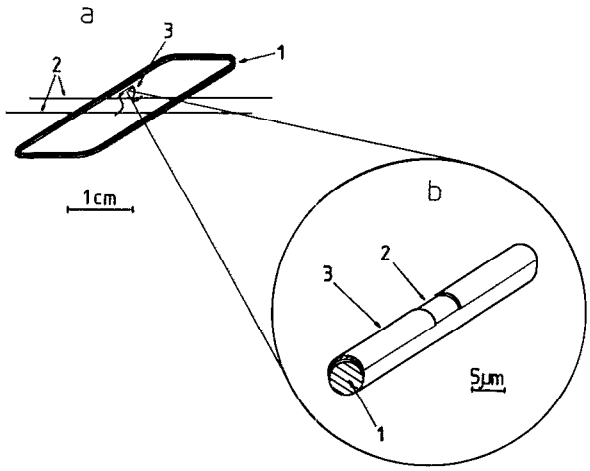

FIG. 1. (a) Schematic diagram of the hot wire anemometer: (1) stainless-steel frame; (2) copper electrical leads; (3) silver wires supporting the glass fiber. (b) Enlarged view of the sensitive part of the detector: (1) glass fiber; (2) resistive Cr film; (3) superconducting Pb-In film.

$$A=\frac{R_1 I^2}{2K_H[\cosh(l/\lambda_1)+(\lambda_1/\lambda_2)\sinh(l/\lambda_1)]},$$

$$B=\frac{R_1 I^2}{K_H[1+(\lambda_2/\lambda_1)\coth(l/\lambda_1)]},$$

where $2l$ is the length of the hot spot, $T_1=T_0+R_1I^2/K_H$; $\lambda_1=\sqrt{K_{Cr}/K_H}$, $\lambda_2=\sqrt{K_s/K_H}$ are the characteristic lengths for the temperature variations along the hot spot and the Pb-In section, respectively. R_1 is the hot spot resistance per unit length. K_{Cr}, the normalized thermal conductivity of chromium and K_s, the normalized thermal conductivity of the superconductor, are assumed constant from 4 K to T_1 for simplicity. The maximum temperature of the wire, reached at $x=0$, is

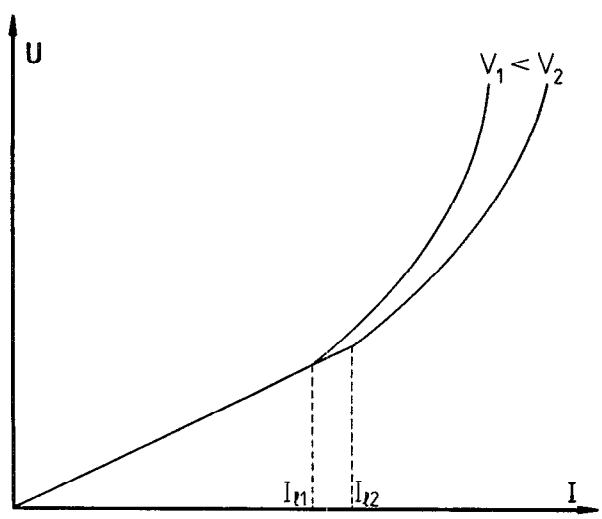

FIG. 2. Voltage-current characteristic for two different flow regimes ($v_2 > v_1$).

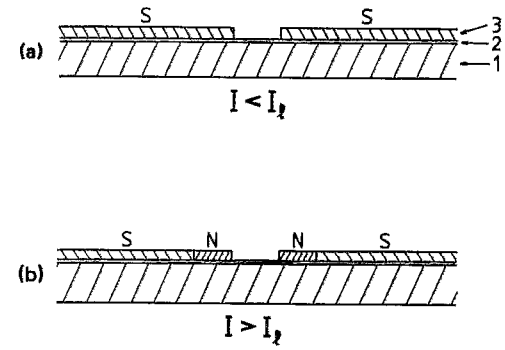

FIG. 3. (a) Cross section of the wire in the superconducting state ($I < I_l$). (b) Cross section of the wire in a partially normal state ($I > I_l$): (1) glass fiber; (2) resistive Cr film; (3) superconducting Pb-In film.

$$T_{\max}=T_0+\frac{R_1I^2}{K_H}\times\left(1-\frac{1}{\cosh(l/\lambda_1)+(\lambda_1/\lambda_2)\sinh(l/\lambda_1)}\right).$$

The critical current I_l is reached when $B=T_c-T_0$, then

$$I_l=\left[\frac{K_H(T_c-T_0)}{R_1}\left(1+\frac{\lambda_2}{\lambda_1}\coth\frac{l}{\lambda_1}\right)\right]^{1/2}. \quad (3)$$

(b) $I>I_l$, the superconductor is partially normal on a length $2(\delta-l)$, that is, $\delta-l$ on each side of the hot spot, with a resistance R_2 per unit length [Fig. 3(b)]. The new temperature profile is given by

$$T=T_1-2C\cosh\frac{x}{\lambda_1} \quad (x\leqslant l),$$

$$T=T_0+De^{(\delta-x)/\lambda_2}-2\frac{R_2I^2}{K_H}\sinh^2\left(\frac{\delta-x}{2\lambda_2}\right) \quad (l\leqslant x\leqslant\delta), \quad (4)$$

$$T=T_0+De^{(\delta-x)/\lambda_2} \quad (x\geqslant\delta),$$

with the same notations previously used. The only approximation is to consider that the Pb-In thermal conductivity is temperature independent in the operating range, no matter its normal or superconducting state. C and D are coefficients from which it is possible to calculate the value of I at a given δ. The transition ($T=T_c$) occurs at $x=\delta$ and the corresponding current I_δ is given by

$$I_\delta=I_l e^{y/2}\left[1+\frac{R_2}{R_1}\left(\frac{\lambda_2}{\lambda_1}\coth\frac{l}{\lambda_1}\sinh y+2\sinh^2\frac{y}{2}\right)\right]^{-1/2}, \quad (5)$$

where $y=(\delta-l)/\lambda_2$.

Let us come now to a few words about the dynamical response. It can be discussed by adding a term to Eq. (1):

$$RI^2=-K_M\,\partial^2T/\partial x^2+K_H(T-T_0)+C\,\partial T/\partial t. \quad (1')$$

C is the heat capacity per unit length of the wire. After a perturbation, for long enough time t, the temperature profile relaxes towards the equilibrium one $T_{eq}(x)$ as

$$T(x,t)=T_{eq}(x)+\theta(x)\exp(-t/\tau),$$

where τ is the response time which is obtained by solving the θ linearized equation. We give only the result for a symmetric function $\theta(x)$:

$$\tau=\tau_0/(1-\alpha^2), \quad \lambda_i'=\lambda_i/\alpha$$

with $\tau_0=C/K_H$ (C is considered as a constant for simplicity) and

$$\alpha=\frac{R_2\lambda_2}{R_1\lambda_1}\frac{[(\lambda_2/\lambda_1)\coth(l/\lambda_1)+1]}{[(\lambda_2/\lambda_1)\coth(l/\lambda_1')+1]}\coth\frac{l}{\lambda_1}.$$

The order of magnitude of τ is thus given by τ_0, as is clear from the two last term in Eq. (1'). However, the exact result shows that the equilibrium is unstable if $\alpha>1$. It corresponds to the cases where the transition propagates at infinity as soon as it occurs.

With the measured characteristics of our wire, and using standard values of the glass specific heat: $\tau_0\simeq 3\times 10^{-7}$ s. This value is of the same order of magnitude as the shortest fluctuation time we expect in the flow.

III. THE FABRICATION AND CHARACTERIZATION OF THE DETECTOR

The glass fiber is a single filament from a commercial bundle of an "E" borosilica without soda.[4] After cleaning under fluorhydric and nitric acids, the 5-μm-diam wire is rinsed with distilled water. It is glued with silver paint to a couple of silver wires (ϕ 50 μm) being used as connecting wires (Fig. 1). Two layers are then successively thermally evaporated in one run: one of 500 Å of chromium[5] at a rate of 3 Å/s, another, to avoid Cr oxydation, of 100 Å gold or silver[6] at a rate of 2 Å/s, under pressures lower than 10^{-6} Torr. The resistance R_0^T of this first deposit is measured through the classical four wire method at various temperatures T. Resistivities of 50 and 100 $\mu\Omega$ cm have been obtained for two different gold on chromium samples at 300 K. Other samples with 100 Å silver instead of gold have shown resistivity values of the same order of magnitude. In a preliminary experiment, where 1000 Å chromium was deposited, a 100 $\mu\Omega$ cm resistivity was also measured. The ratio $R_0^{300\ \mathrm{K}}/R_0^{4.2\ \mathrm{K}}$ did not exceed 1.15.

From all these tests, several remarks should be pointed out. Chromium is easy to evaporate on glass fibers in thicknesses ranging from 500 to 1000 Å. However, significative resistance variations are observed on short periods when placed in air. To avoid such an aging effect, a layer of noble metal should plate the chromium. Gold has been chosen due to its poor oxidation. The large resistivity observed, five to ten times that of bulk samples, is probably due to the perturbed crystalline character of these thin layers.

Perpendicularly to the chromium-gold sublayer, a fiber glass ($\phi=5$ μm) is placed in order to mask a small area during the next deposit of a superconducting material with 2000–3000 Å typical thicknesses. First tests with pure lead have shown a high thermal conductivity (up to 80 mW cm^{-1} K^{-1} from the electrical resistivity measurement) of the deposit and then a rather poor sensitivity of the detector; moreover, aging effects probably due to oxydation needed a new deposit of silver ($\sim$500 Å thickness).

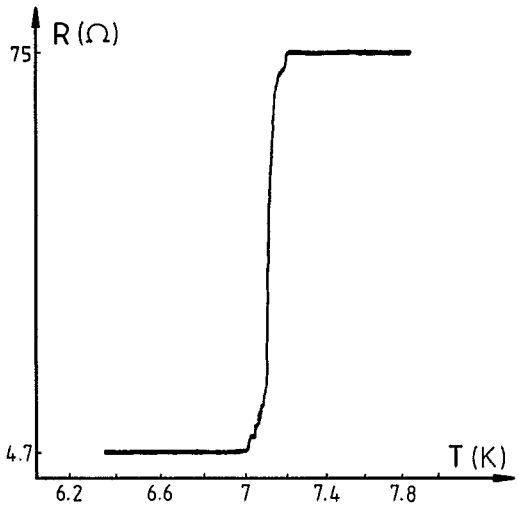

FIG. 4. Resistance vs temperature of a 2800 Å $Pb_{0.8}In_{0.2}$ detector.

Tentatives with niobium deposition appeared quite difficult. Finally, excellent results have been obtained by using lead-indium alloys with concentrations in the range 20%–35% atomic indium measured through electron microprobe microanalysis.[7]

ac four wires measurements of a typical detector resistance are shown in Fig. 4 versus temperature. Varying from 4.7 Ω at 4.2 K to 75 Ω above 7.2 K, the recorded values have to be compared with the 237 Ω resistance at room temperature. At 300 K, before beeing coated with the superconductor, the chromium-gold sublayer exhibited a 1590 Ω value. The length of the detector is 920 μm and then the estimated residual 4.2 K value should correspond to a hot spot length: $2l\sim 3$ μm. However, observation under microscope exhibits steps in the deposit at $2l=5$ μm. The difference between the estimated and observed values may originate from inhomogeneities in the chromium-gold deposit. Shadowing effects during the Pb-In evaporation may also reduce the hot spot resistance due to a low thickness coverage of this region with the superconducting layer. In this case this area should still have a rather high resistance per unit length and thus R_1 should not be significantly modified. In the following calculations we have used the $2l=5$ μm observed value.

The roundoffs on the R-T characteristics around T_c (Fig. 4) are possibly due to the experimental setup, where the T measurement is done through a carbon resistor averaging the gas temperature a few millimeters away from the detector.

The resistivity value of the Pb-In alloy in the normal state is 11 $\mu\Omega$ cm for this deposit with an estimated layer width equal to the diameter of the glass fiber and a 2800 Å thickness. The thermal conductivity of the Pb-In layer, $k_s=16$ mW cm^{-1} K^{-1}, is deduced using the Wiedeman–Franz law. For one 35% In concentration, a k_s value of 9 mW cm^{-1} K^{-1} has been obtained.

IV. DISCUSSION OF THE RESULTS

We will now use the formalism of Sec. II to compare the experimental results with the calculated ones. We have

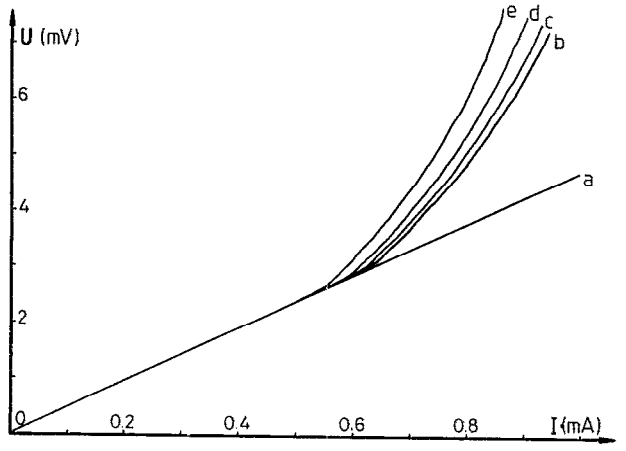

FIG. 5. Measured voltage—dc current characteristic of the detector at various temperatures: Detector in liquid He: (a) $T=4.2$ K. Detector in gaseous He: (b) $T=4.3$ K; (c) $T=4.4$ K; (d) $T=4.6$ K; (e) $T=4.9$ K.

defined the normalized thermal conductivities of both the chromium and the superconducting regions K_{Cr} and K_s. The thermal conductivity k_{fg} of the fiber glass has also to be taken into account. Then

$$K_{Cr}=k_{Cr}\times A_{Cr}+k_{fg}\times A_{fg}\sim 2\times 10^{-10}\ \text{W cm K}^{-1},$$

$$K_s=k_s\times A_s+k_{Cr}\times A_{Cr}+k_{fg}\times A_{fg}\sim 4\times 10^{-10}\ \text{W cm K}^{-1},$$

$$K_H\simeq \pi k_{He}\simeq 3\times 10^{-4}\ \text{W cm}^{-1}\,\text{K}^{-1}\ \text{for zero velocity,}$$

with k_{fg} and k_{He} from Ref. 8.

The calculated values $\lambda_1=8$ μm and $\lambda_2=12$ μm are rather large and strongly dependent on the glass fiber diameter. For given sizes and layer thicknesses, they only depend on K_H, that is, of the gas velocity. Along the hot spot, the temperature is more or less constant and the temperature decreases slowly further.

From $R_1=9.4\times 10^3$ Ω/cm and a mean critical temperature $T_c=7.2$ K, the expected critical current is deduced from Eq. (3): $I_l=0.75$ mA in good agreement with the 0.62 mA measured value (Fig. 5) taking into account the uncertainty on the K_H value. The temperature along the hot spot should vary from 7.8 K to 7.2 K when I_l is applied. This will be discussed further.

The I_δ value for a transition of the superconductor to the normal state on a length $2(\delta-l)$ may also be determined. For $\delta-l=5$ μm with $R_2=7.7\times 10^2$ Ω/cm, $I_\delta=0.85$ mA. This 14% current variation confirms the high sensitivity $d(\delta-l)/dI$ of the detector, already observed in the characterization measurements.

Using the set of Eq. (4) some dependences of the characteristics of the anemometer have been examined.

First the current I_∞ flowing in the detector, when the whole transition to the normal state occurs, is given by

$$I_\infty=I_l\left[\frac{R_2}{2R_1}\left(\frac{\lambda_2}{\lambda_1}\coth\frac{l}{\lambda_1}+1\right)\right]^{-1/2}=\left[\frac{2K_H(T_c-T_0)}{R_2}\right]^{1/2}.$$

In our particular case: $I_\infty=1.53$ mA about twice the critical current I_l. The sensitivity $d(\delta-l)/dI$ is more or less constant (~ 50 μm/mA) from the smaller values of $\delta-l$ up to $\delta=25$ μm. For $\delta=50$ μm, $I_\delta=0.96\ I_\infty$ and this sensitivity essentially diverges.

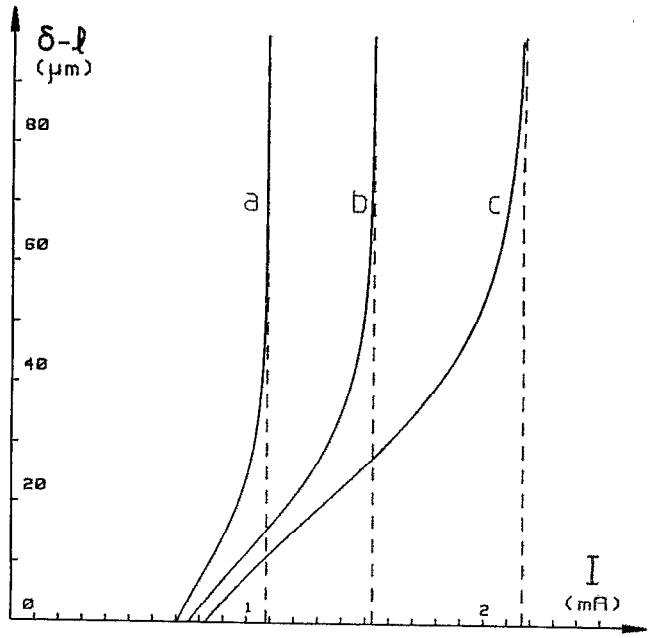

FIG. 6. Calculated normal state length of the superconducting material vs the applied current for three superconductor thicknesses: (a) 1400 Å; (b) 2800 Å (thickness of the measured anemometer); (c) 5600 Å.

A second remark is that the thinner the Au-Cr layer the smaller $d(\delta-l)/dI$. In fact the decrease of this thickness corresponds to a higher dissipation in the hot spot and then a decrease of I_l, while I_∞ which depends only on R_2 is independent of this parameter. A similar remark holds for the $d(\delta-l)/dI$ dependence on the hot spot length.

Reversely, as seen in Fig. 6, the thicker the superconducting layer, the smaller $d(\delta-l)/dI$. In that case the increase of K_s is small due to the large contribution of the fiber glass compared to that of the superconductor. However, the inverse linear variation of R_2 with the thickness gives rise to a large increase of I_∞. With variations of the critical temperature in the 6–8 K range the effects are simply homothetics.

The voltage across the detector is given by

$$V=2I_\delta(lR_1+y\lambda_2R_2),$$

with $y=(\delta-l)/\lambda_2$.

At first order, for small y

$$I_\delta=I_l\left[1+\frac{y}{2}\left(1-\frac{\lambda_2R_2}{\lambda_1R_1}\coth\frac{l}{\lambda_1}\right)\right]$$

and

$$V=2lR_1I_\delta+\frac{4R_2\lambda_2(I_\delta-I_l)}{1-(\lambda_2R_2/\lambda_1R_1)\coth(l/\lambda_1)}\frac{I_\delta}{I_l}.$$

Such a quadratic behavior with a change of slope at I_l is suggested on the curves of Fig. 5.

The temperature profile is presented in Fig. 7 for three different values of the current. λ_2 governs the relaxation to the thermal bath temperature T_0. Even with a large current

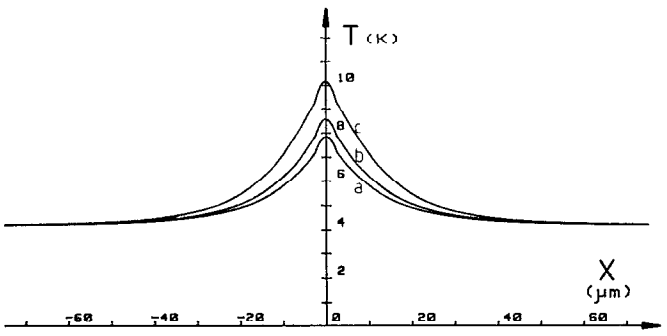

FIG. 7. Calculated temperature profile along the detector for three different values of the current: (a) $I=I_l$; (b) $I=1.065I_l$; (c) $I=1.2I_l$.

the temperature of the hot spot is more or less constant within 0.7 K at most. This is due to the large λ_1 value compared to l.

In the previous discussion, the velocity field is assumed constant at a given time t all along the detector. If some local velocity fluctuation occurs, a relative cooling or heating of the wire will respectively rise or decrease the critical current. Such a perturbation has been simulated by calculating the rise of the critical current due to a 50% local, square shape, increase of the normalized heat transfer coefficient K_H. The results on Fig. 8 show the relative increase of the critical current as a function of x, the distance between the middle position of the square shape perturbation and the middle of the detector hot spot for three different perturbation lengths l_p. Even a low l_p value of 5 μ will modify I_l by 5%. The localized character of the detector is easily observable. As soon as the perturbation does not overlap the hot spot completely, the rise in I_l drops severely down. A 1–2 μ diameter wire will reduce the λ_1 and λ_2 values and then allows the detector to meet the requirements initially discussed.

Let us finally present the results showing the high dynamical response of our prototype wire. The way the measurements are made is close to the standard "constant temperature" mode.

The dissipation of a "dc" current i_{dc} allows the resistance of the wire to be equal to a reference one to which it

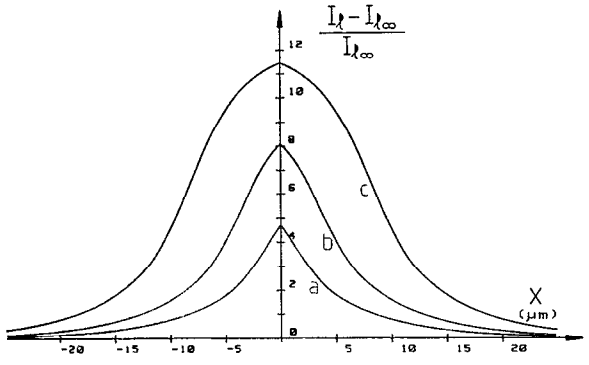

FIG. 8. Simulation of a perturbation in the velocity field for three perturbation lengths: (a) 5 μ; (b) 10 μ; (c) 20 μ. The perturbation is assumed to increase the heat exchange coefficient K_H by 50%. I_{l_∞} is the value of I_l when the perturbation is far from the hot point.

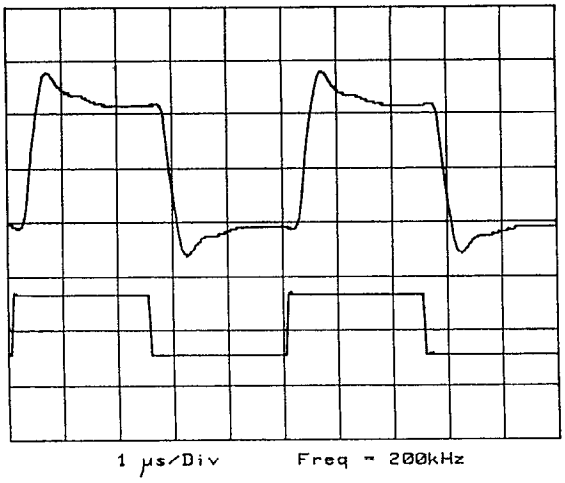

FIG. 9. Response to a 200 kHz squarewave perturbation of the electrical dissipated power.

is compared through a 10 MHz bridge.[9] i_{dc} adapts itself to the fluctuations of K_H and is thus our "measure" of the flow velocity. We have externally added a square-wave signal to i_{dc} and looked at the reaction of the apparatus. In about 1.5 μs the detected signal comes to its equilibrium value as seen in Fig. 9 for a 200 kHz applied perturbation. It is important to mention that, while in a constant temperature operation, we still have a response time of the order of magnitude of the wire thermal one: conventional hot wire setups can reach two orders of magnitude improvement compared to their thermal response time.[10] Here it has been seen that the very low heat capacity of the wire gives unusual high intrinsic response time. To go higher will be limited by propagation effects in connecting wires.

V. DISCUSSION

The present hot wire shows large impedances suitable for anemometry experiments. From a simple heat transfer model the behavior of the detector has been studied for a constant velocity configuration and also with a perturbation simulating the turbulent character of the flow. This study confirms the possibility of fast response and very localized character of such detectors which give access to the small characteristic scales of energy dissipation occurring in this problem.

ACKNOWLEDGMENTS

The authors are grateful to J. Chaussy, M. Giroud, B. Pannetier for numerous discussions and help and to J. Geneste for his technical assistance.

APPENDIX

The temperature profile in the detector is obtained from the local energetic equation

$$RI^2 = -K_M \frac{d^2T}{dx^2} + K_H(T - T_0), \tag{1}$$

where T is the temperature at the distance x from the middle of the hot spot.

Two cases have to be considered depending on the current flowing in the detector:

A. Temperature profile if no transition occurred in the superconductor ($I<I_l$)

1. In the hot spot region ($x<l$)

$$K_H T - K_{Cr}\frac{d^2T}{dx^2} = K_H T_0 + R_1 I^2.$$

The general solution is

$$T = T_0 + \frac{R_1 I^2}{K_H} + \Delta_+ e^{x/\lambda_1} + \Delta_- e^{-x/\lambda_1},$$

with $\lambda_1 = \sqrt{K_{Cr}/K_H}$.

For symmetry reasons

$$T(x=0) = T_{\max} \quad \text{and} \quad \left.\frac{dT}{dx}\right|_{x=0} = 0.$$

Then $\Delta_+ = \Delta_- = -A$ (A has to be positive due to the fact that $d^2T/dx^2 < 0$) and

$$T = T_0 + \frac{R_1 I^2}{K_H} - 2A\cosh\frac{x}{\lambda_1}.$$

2. In the superconducting region ($x>l$)

$$R = 0 \quad \text{and} \quad K_H T - K_s\frac{d^2T}{dx^2} = K_H T_0$$

It follows

$$T = T_0 + Be^{(l-x)/\lambda_2},$$

with $\lambda_2 = \sqrt{K_s/K_H}$.

In order to determine the values of the A and B constants two conditions have to be fulfilled at the hot spot-superconductor border ($x=l$):

a. The temperature continuity

$$T_0 + \frac{R_1 I^2}{K_H} - 2A\cosh\frac{l}{\lambda_1} = T_0 + B.$$

b. The thermal flux continuity

$$K_{Cr}\left(\frac{dT}{dx}\right)_{x=l-0} = K_s\left(\frac{dT}{dx}\right)_{x=l+0}$$

then

$$-\frac{2A}{\lambda_1}K_{Cr}\sinh\frac{l}{\lambda_1} = -\frac{K_s B}{\lambda_2}$$

and

$$B = 2A\frac{\lambda_1}{\lambda_2}\sinh\frac{l}{\lambda_1}.$$

It follows

$$A = \frac{R_1 I^2}{2K_H}\left(\cosh\frac{l}{\lambda_1} + \frac{\lambda_1}{\lambda_2}\sinh\frac{l}{\lambda_1}\right)^{-1},$$

$$B = \frac{R_1 I^2}{K_H}\left(1 + \frac{\lambda_2}{\lambda_1}\coth\frac{l}{\lambda_1}\right)^{-1}.$$

B. Temperature profile when the transition has occurred on the length $\delta - l$ ($I>I_l$)

1. In the hot spot region ($x<l$)

Again

$$T = T_0 + \frac{R_1 I^2}{K_H} - 2C\cosh\frac{x}{\lambda_1}.$$

2. For $l<x<\delta$

$$K_H T - K_s\frac{d^2T}{dx^2} = K_H T_0 + R_2 I^2$$

then

$$T = T_0 + \frac{R_2 I^2}{K_H} + \Delta_{N+} e^{(l+x)/\lambda_2} + \Delta_{N-} e^{(l-x)/\lambda_2}.$$

3. For $x>\delta$

$R=0$, then

$$K_H T - K_s\frac{d^2T}{dx^2} = K_H T_0,$$

$$T = T_0 + De^{(\delta-x)/\lambda_2}.$$

To find the values of C, D, Δ_{N+}, and Δ_{N-} the temperatures and thermal flux continuities have now to be written for both $x=l$ and $x=\delta$.

a. The temperature continuity

*$x=l$:

$$T_0 + \frac{R_1 I^2}{K_H} - 2C\cosh\frac{l}{\lambda_1} = T_0 + \frac{R_2 I^2}{K_H} + \Delta_{N+} e^{2l/\lambda_2} + \Delta_{N-}, \tag{A1}$$

*$x=\delta$ and $T=T_c$, then $D = T_c - T_0$

and

$$D = \frac{R_2 I^2}{K_H} + \Delta_{N+} e^{(l+\delta)/\lambda_2} + \Delta_{N-} e^{(l-\delta)/\lambda_2}. \tag{A2}$$

b. The heat flux continuity

*$x=l$: $$K_{Cr}\left(\frac{dT}{dx}\right)_{x=l-0} = K_s\left(\frac{dT}{dx}\right)_{x=l+0},$$

$$-2C\frac{K_{Cr}}{\lambda_1}\sinh\frac{l}{\lambda_1} = K_s\left(\frac{\Delta_{N+}}{\lambda_2}e^{2l/\lambda_2} - \frac{\Delta_{N-}}{\lambda_2}\right), \tag{A3}$$

*$x=\delta$: $$K_s\left(\frac{dT}{dx}\right)_{x=\delta-0} = K_s\left(\frac{dT}{dx}\right)_{x=\delta+0}$$

then

$$\frac{\Delta_{N+}}{\lambda_2}e^{(l+\delta)/\lambda_2} - \frac{\Delta_{N-}}{\lambda_2}e^{(l-\delta)/\lambda_2} = -\frac{D}{\lambda_2}. \tag{A4}$$

From Eqs. (A2) and (A4):

$$\Delta_{N-}=\left(D-\frac{R_2I^2}{2K_H}\right)e^{(\delta-l)/\lambda_2},$$

$$\Delta_{N+}=-\frac{R_2I^2}{2K_H}e^{(l-\delta)/\lambda_2}.$$

And from Eq. (A1),

$$2C\cosh\frac{l}{\lambda_1}=\frac{R_1I^2}{K_H}+\frac{2R_2I^2}{K_H}\sinh^2\frac{(l-\delta)}{2\lambda_2}-(T_c-T_0)e^{(\delta-l)/\lambda_2}.$$

[1] D. C. Threlfall, J. Fluid Mech. **67**, 17 (1975).

[2] B. Castaing, G. Gunaratne, F. Heslot, L. Kadanoff, A. Libchaber, S. Thomae, X. Z. Wu, S. Zaleski, and G. Zanetti, J. Fluid Mech. **204**, 1 (1989).

[3] For more information see, for example, G. Comte-Bellot, J. Phys. (Paris) Colloq. **37**, C1-67 (1976), and references therein.

[4] Vetrotex-S[t] Gobain, 767 Quai des Allobroges, 73009 Chambery.

[5] The evaporated Cr rods are from R. D. Mathis part number CRW-1.

[6] The evaporated Au 1 mm wire and 5 μ Ag rod are from Comptoir Lyon Allemand part number Purela HP and from Johnson Matthey, respectively.

[7] The measurement was made with the help of T. Fournier.

[8] R. R. Conte, in *Eléments de Cryogénie*, edited by Masson (1970).

[9] J. P. Faure and J. L. Bret (unpublished).

[10] P. Freymuth, J. Phys. E **10**, 705 (1977).